The Relativistic Boltzmann Equation

Maitraya Bhattacharyya

Max-Planck-Institut für Astronomie, Heidelberg, Germany

[with David Radice & Yi Qiu]

AthenaK Summer School 2026

July 13, 2026

GW170817

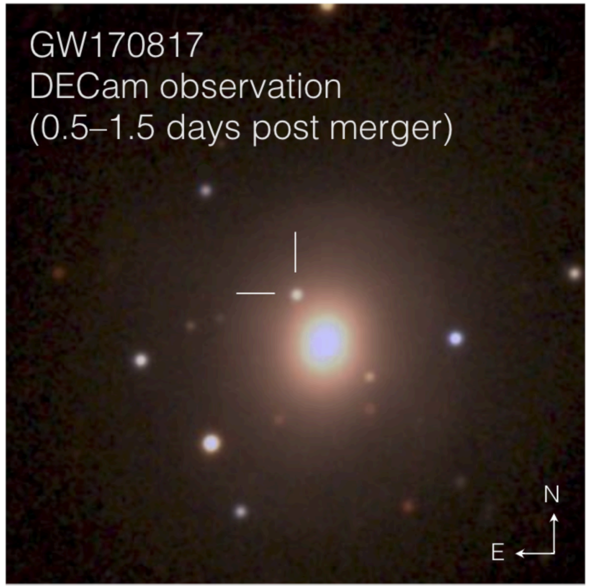

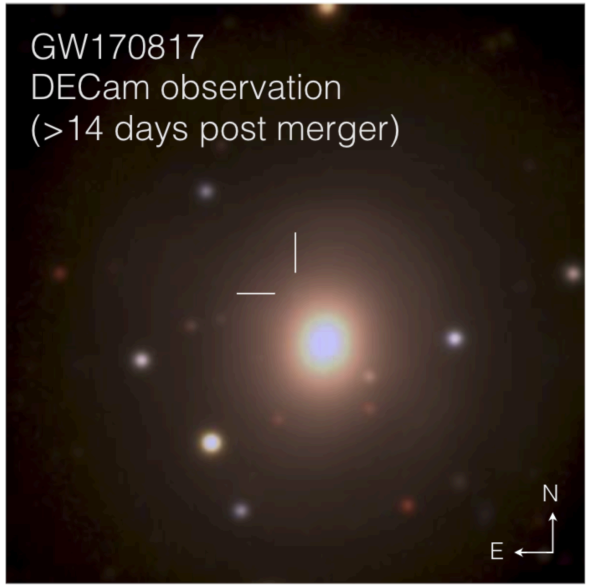

NGC 4993: optical counterpart of GW170817, 0.5-1.5 days, 2 weeks [Soares-Santos+ 2017]

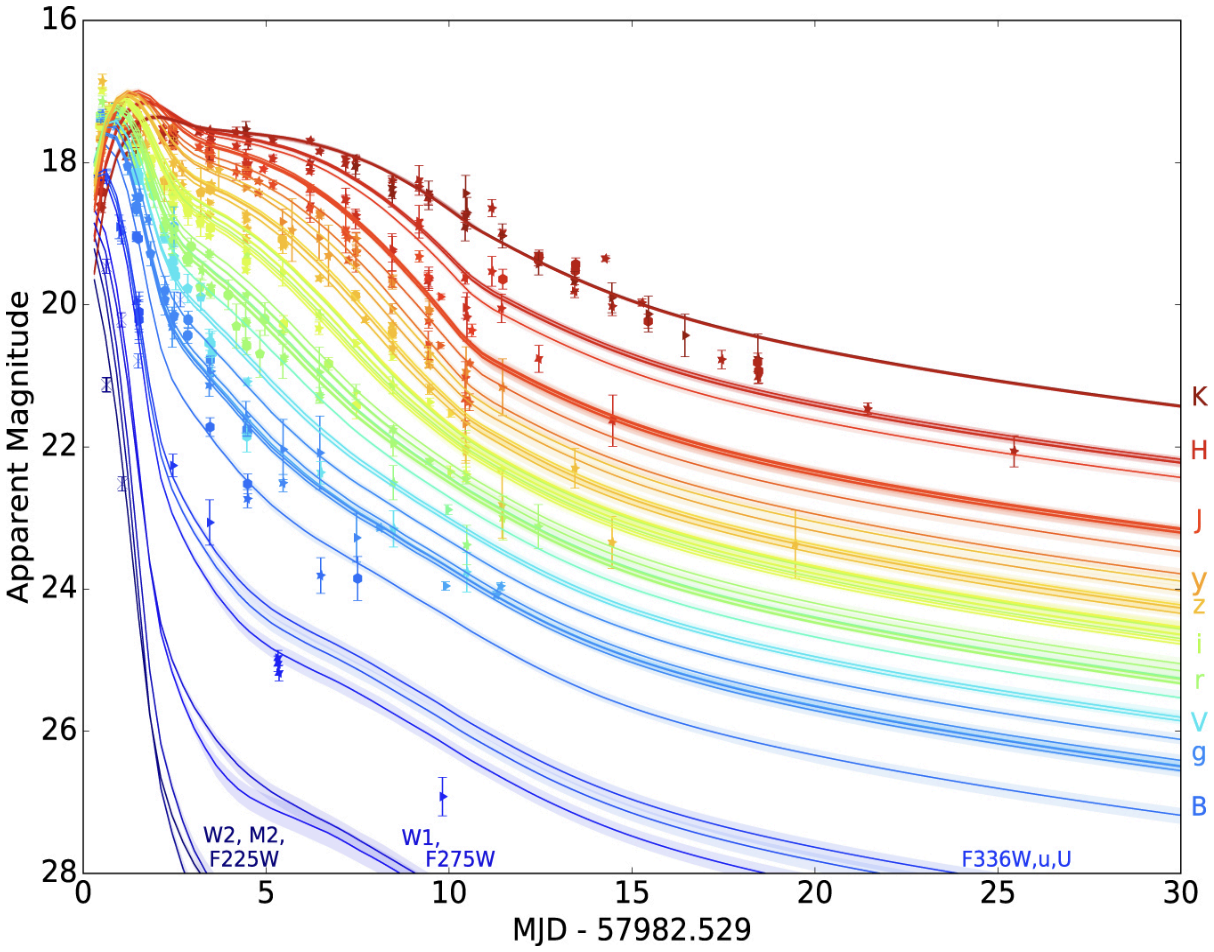

UVOIR light curves [Villar et. al. 2017]

Why transport? Neutrinos set the composition

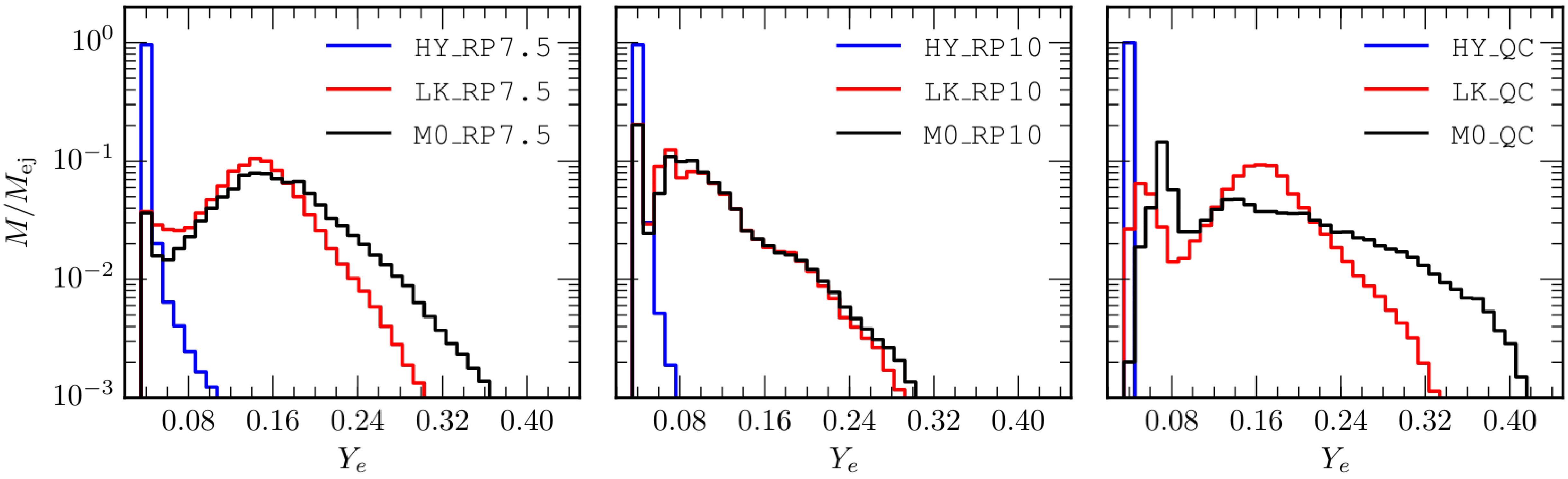

Ejecta Y_e with **no neutrinos (HY)**, **leakage (LK)**, **moment transport (M0)** for three configurations [Radice+ 2016]

Roadmap

The equation

The GR Boltzmann equation and why it's hard

Exact methods

FP_N / FEM_N full-Boltzmann solvers

M1

Moment based methods in AthenaK

Specific intensity and the distribution function

Radiation field described by specific intensity I, defined s.t. **[Mihalas & Mihalas 1984]**

$$\mathrm{d}E = I\,\cos\theta\,\mathrm{d}A\,\mathrm{d}\nu\,\mathrm{d}\Omega\,\mathrm{d}t$$

is the radiation energy in

- frequency ranges ν and $\nu + d\nu$
- traveling in Ω direction b/w solid angle $d\Omega$
- crossing time interval dt
- an area element $\mathrm{d}A$ with unit normal $\mathbf{n}$

with θ being angle between $\mathbf{n}$ and the propagation direction $\mathbf{\Omega}$

Neutrinos treated as **massless**

$$p^\mu = \frac{h\nu}{c}\,(1,\,\mathbf{n}), \qquad p_\mu p^\mu = 0$$

$$\mathbf{n} = (\sin\theta\cos\phi,\ \sin\theta\sin\phi,\ \cos\theta)$$

Momentum fixed by energy $\varepsilon = h\nu$ and direction (θ, ϕ)

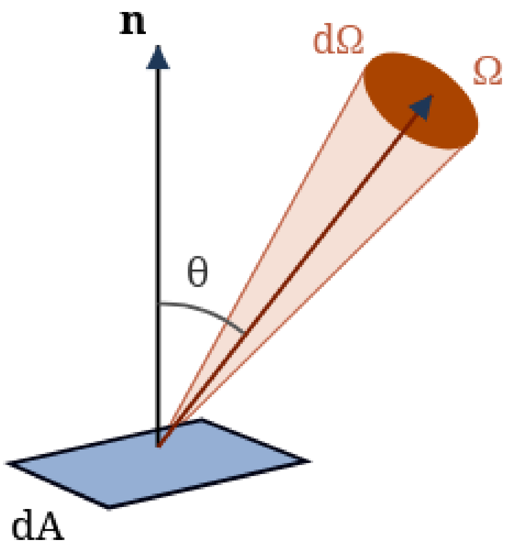

F is the **Lorentz-invariant** distribution function:

$$\mathrm{d}N = F\,p^\mu t_\mu\,\mathrm{d}^3x\,\frac{\mathrm{d}^3p}{-p_0} = \frac{h^3\nu^2}{c^2}\,F\,\mathrm{d}^3x\,\mathrm{d}\nu\,\mathrm{d}\Omega$$

Here t_μ is the unit vector normal to the $t =$const slice and $\mathrm{d}^3p/(-p_0)$ is the invariant momentum-space volume element. Each carrier moves energy $h\nu$, so $\mathrm{d}E = h\nu\,\mathrm{d}N$:

$$\boxed{I = \frac{h^4\nu^3}{c^2}\,F}$$

The Boltzmann equation

Sans collisions, F follows a geodesic flow in phase space. In the presence of collisions:

$$\frac{\mathrm{d}F}{\mathrm{d}\lambda} = \mathbb{C}[F]$$

where λ: affine parameter, $\mathbb{C}[F]$: is the collision term. **[Cardall+ 2013]**

Now parametrize phase space by the spacetime cordinates x^μ and momentum p^i (independent components only).

The chain rule then gives

$$\frac{\mathrm{d}x^\mu}{\mathrm{d}\lambda}\frac{\partial F}{\partial x^\mu} + \frac{\mathrm{d}p^i}{\mathrm{d}\lambda}\frac{\partial F}{\partial p^i} = \mathbb{C}[F]$$

The geodesic equation for particle trajectories is given by

$$\frac{\mathrm{d}x^\mu}{\mathrm{d}\lambda} = p^\mu, \qquad \frac{\mathrm{d}p^\mu}{\mathrm{d}\lambda} = -\Gamma^\mu{}_{\nu\rho}\, p^\nu p^\rho$$

Substituting geodesic equations gives the GR Boltzmann equation

$$\boxed{p^\mu \frac{\partial F}{\partial x^\mu} - \Gamma^i{}_{\nu\mu}\, p^\nu p^\mu \frac{\partial F}{\partial p^i} = \mathbb{C}[F]}$$

The equation is valid in any coordinates, but must choose frame to evaluate $\mathbb{C}[F]$ and the connection coefficients Γ.

Which frame?

- Spacetime position stays in lab frame, since multi-D fluid solvers are Eulerian
- The collision term is simple only in the frame where matter is at rest, since that is where the interacting species reach an isotropic equilibrium
- The mass shell and its momentum volume element depend on position, since the metric can only be diagonalized to Minkowski form locally, so no fixed global momentum grid exists in curved spacetime

Measuring momenta in an **orthonormal tetrad comoving with the fluid** solves both problems at once. Since this tetrad is locally Minkowski, the flat spacetime results of special relativity carry over directly into the collision integral **[Cardall+ 2013]**.

The tetrad frame and the BE

Notation [Cardall+ 2013]

- lab coordinates use simple indices, x^μ, the coordinate basis tied to the lab or Eulerian frame
- comoving coordinates use hatted indices, $p^{\hat\mu}$, momentum components in the orthonormal frame carried by the fluid
- comoving curvilinear coordinates use tilded indices, $p^{\tilde\imath} = (\varepsilon, \theta, \varphi)$

Choose four orthonormal vectors $L^\mu{}_{\hat\mu}$, a **tetrad**, with the time leg on the fluid, built by Gram-Schmidt from $(u^\mu, \partial_x, \partial_y, \partial_z)$

$$L^\mu{}_{\hat 0} = u^\mu, \qquad L^\mu{}_{\hat\mu} L^\nu{}_{\hat\nu}\, g_{\mu\nu} = \eta_{\hat\mu\hat\nu}$$

$L^\mu{}_{\hat\mu}$ is the transformation matrix between the lab coordinate basis and the comoving orthonormal frame, with $\det L = (-g)^{-1/2}$

Since F is a scalar, rewriting its derivatives as covariant ones

$$p^{\hat\mu} L^\mu{}_{\hat\mu}\, \nabla_\mu F - \Gamma^{\hat\imath}{}_{\hat\nu\hat\mu}\, p^{\hat\nu} p^{\hat\mu}\, P^{\tilde\imath}{}_{\hat\imath}\, D_{\tilde\imath} F = \mathbb{C}[F]$$

Expanding by the product rule turns both terms into divergences

$$\boxed{\frac{1}{\sqrt{-g}} \frac{\partial}{\partial x^\mu} \left[\sqrt{-g}\, L^\mu{}_{\hat\mu}\, p^{\hat\mu} F \right] + \frac{(-p_{\hat 0})}{\sqrt{\lambda}} \frac{\partial}{\partial p^{\tilde\imath}} \left[- \frac{\sqrt{\lambda}}{(-p_{\hat 0})}\, P^{\tilde\imath}{}_{\hat\imath}\, \Gamma^{\hat\imath}{}_{\hat\nu\hat\mu}\, p^{\hat\nu} p^{\hat\mu} F \right] = \mathbb{C}[F]}$$

- the first term is a **spacetime divergence** and second term is a **momentum space divergence**
- the Jacobian $P^{\tilde\imath}{}_{\hat\imath} = \partial p^{\tilde\imath} / \partial p^{\hat\imath}$ and the comoving connection coefficients $\Gamma^{\hat\imath}{}_{\hat\nu\hat\mu}$ redistribute carriers in energy and angle, with $\sqrt{\lambda} = \varepsilon^2 \sin\theta$ the momentum space volume element
- both divergence terms, so the form is **manifestly conservative**, with conserved density $\sqrt{-g}\, L^0{}_{\hat\mu} p^{\hat\mu} F$, the Eulerian carrier number density

Neutrino emission and absorption

Emission and absorption enter as source terms along the trajectory

$$\frac{\mathrm{d}F}{\mathrm{d}\lambda} = \eta - \frac{1}{\lambda_a} F$$

with η the emissivity and λ_a the absorption mean free path.

Introducing the **source function** $S \equiv \lambda_a \eta$ turns this into a relaxation equation

$$\frac{\mathrm{d}F}{\mathrm{d}\lambda} = \frac{1}{\lambda_a} \left[S - F\right]$$

so matter drives the radiation field toward S within a few mean free paths, $F \to S$ once $\ell \gg \lambda_a$.

For thermal processes, in the frame comoving with the medium, S is the blackbody function

$$\boxed{S = \frac{g}{h^3} \frac{1}{e^{(\varepsilon-\mu)/kT} + 1} =: B}$$

In a frame where the medium moves, S keeps this form but with $\varepsilon = \varepsilon(p, v)$, so the equilibrium function becomes anisotropic there. This is the practical reason collision terms are evaluated in the comoving frame.

Neutrino scattering

Scattering moves carriers between momenta, an integral operator

$$\frac{\mathrm{d}F}{\mathrm{d}\lambda} = \int \sigma(p' \to p)\, F(p')\, \sqrt{-g}\, \frac{\mathrm{d}^3 p'}{-p'_0} - \int \sigma(p \to p')\, F(p)\, \sqrt{-g}\, \frac{\mathrm{d}^3 p'}{-p'_0}$$

The simplest closure of the kernel, **isotropic and elastic** scattering,

$$\sigma(p' \to p) = \tfrac{1}{4\pi\varepsilon\lambda_s}\, \delta(\varepsilon - \varepsilon')$$

gives a relaxation toward the angular average

$$\frac{\mathrm{d}F}{\mathrm{d}\lambda} = \frac{1}{\lambda_s}\left[\langle F\rangle - F\right] \qquad \Longrightarrow \qquad F \to \langle F\rangle \text{ once } \ell \gg \lambda_s$$

The Boltzmann equation with collision terms

$$\frac{\mathrm{d}F}{\mathrm{d}\lambda} = p^\mu \frac{\partial F}{\partial x^\mu} - \Gamma^i{}_{\alpha\beta} p^\alpha p^\beta \frac{\partial F}{\partial p^i} = \underbrace{\frac{1}{\lambda_a}[S - F]}_{\text{emission / absorption}} + \underbrace{\frac{1}{\lambda_s}[\langle F\rangle - F]}_{\text{scattering}} = \mathbb{C}[F]$$

The price of this simplification: energy exchange and scattering anisotropy are discarded.

bns_nurates

Reactions implemented [Bruenn 1985; Burrows+ 2006; Chiesa, MB+ 2025]

- β-processes

$$p + e^- \leftrightarrow n + \nu_e \,, \qquad n + e^+ \leftrightarrow p + \bar{\nu}_e$$

- pair processes and Bremsstrahlung

$$e^- + e^+ \leftrightarrow \nu + \bar{\nu} \,, \qquad N + N \leftrightarrow N + N + \nu + \bar{\nu}$$

- iso-energetic scattering on nucleons, **inelastic** scattering on $e^\pm$

$$N + \nu \to N + \nu \,, \qquad e^\pm + \nu \to e^\pm + \nu$$

- corrections: weak magnetism and recoil, mean-field shifts of nucleon masses and interaction potentials

Library design [Chiesa, MB+ 2025]

- reaction kernels as truncated **Legendre expansions**, integrated on the fly – no interpolation tables
- outputs both **spectral** rates $j(\varepsilon)$, $\lambda^{-1}(\varepsilon)$ and **gray M1 sources** (η, κ_a for energy and number, κ_s)
- neutrino distribution reconstructed from the evolved moments: trapped Fermi-Dirac + free-streaming component
- C++ with **Kokkos** – runs on GPUs inside AthenaK and THC_M1

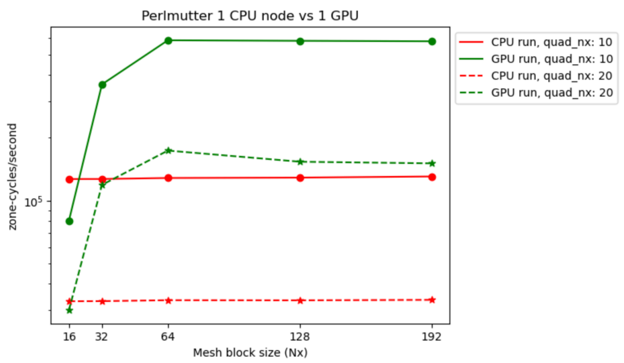

Zone-cycles/s, CPU vs GPU [Chiesa, MB+ 2025]

github.com/RelNucAs/bns_nurates

Why its hard to solve BE

$$F = F(t,\ x^i,\ \varepsilon,\ \theta,\ \phi)$$

a function of **six plus one dimensions**: time, three spatial coordinates, and three momentum coordinates

Dimensionality	Every hydrodynamic cell carries a full energy and angle grid on top of it.
Stiffness	The collision term has to be treated implicitly.
Positivity	$F \geq 0$ has to survive the discretization.
Two-way coupling	Radiation exchanges energy and momentum with the fluid through S^μ, so the two must be evolved together.
Dynamic range	The optical depth $\tau = L/\lambda$ spans $\ll 1$, streaming beams, to $\gg 10^6$, stiff diffusion.

Approximate and exact methods

Approximate methods

- Phenomenological models like neutrino **leakage** schemes [van Riper & Lattimer 1981; Ruffert+ 1996]
- Moment based methods (M1): rewrite the Boltzmann equation in terms of moments of F
- Evolve the first two moments and use a closure to complete the system [Arnett 1977; Foucart+ 2015; Radice+ 2022]
- Accuracy depends on the choice of closure [Garrett & Hauck 2013]

Exact methods

- Monte Carlo methods [Fleck & Cummings 1971]
- Discrete ordinates (S_N) [Mihalas & Mihalas 1984] → “ray effects”, need filtering [Hauck 2019]
- Filtered spherical harmonics (FP_N) [McClarren & Hauck 2010; Radice+ 2013]
- Finite volume/S_N in angle [White+ 2023] See Lizhong’s talk!
- Finite element in angle (FEM_N) [Bhattacharyya & Radice 2023]

Monte-Carlo + M1 [Izquierdo+ 2023]

	Leakage	M1	S_N	FP_N	FEM_N	Monte-Carlo
vars	optical-depth estimate	moments E, F^i	F along N directions	coefficients F^{lm}	F at grid vertices	packets
Boltzmann ?	nope	nope – closure	yes	yes	yes	yes, as $N_p^{-1/2}$
positivity	–	yes	yes	filtering	clipping limiter	yes
problems	no transport at all	crossing beams merge	ray effects	Gibbs oscillations	beam broadening at low N	noise
relative cost	negligible	low	high	high	high	highest when thick

Each method has advantages and disadvantages!

Discretizing the BE

Expand F in a **product basis** of angular and energy functions:

$$F = F^{(A,n)}\,\psi_A(\theta,\phi)\,\chi_n(\varepsilon)$$

We will discuss the specific choice of ψ_A. Energy basis χ_n a piecewise-constant “multigroup” indicator on bins $[\varepsilon_n, \varepsilon_{n+1}]$:

$$\chi_n(\varepsilon) = \begin{cases} 1, & \varepsilon \in [\varepsilon_n, \varepsilon_{n+1}] \\ 0, & \text{otherwise} \end{cases}, \qquad V^{(n)} = \int_{\varepsilon_n}^{\varepsilon_{n+1}} \varepsilon^2 \, d\varepsilon = \tfrac{1}{3}\left(\varepsilon_{n+1}^3 - \varepsilon_n^3\right)$$

Insert into the BE and project with test functions $\psi^B \chi^m$, the discretized system is:

$$\boxed{\frac{1}{\sqrt{-g}}\frac{\partial}{\partial t}\left(\sqrt{-g}\,L^0{}_{\hat\mu}\,F^{(A,n)}\right) V^{(n)} P^{\hat\mu}{}_A{}^B + \frac{1}{\sqrt{-g}}\frac{\partial}{\partial x^\mu}\left(\sqrt{-g}\,L^\mu{}_{\hat\mu}\,F^{(A,n)}\right) V^{(n)} P^{\hat\mu}{}_A{}^B + \Gamma^{\hat\imath}{}_{\hat\nu\hat\mu}\,F^{(A,n)}\,V^{(n)}\,F^{\hat\nu\hat\mu}{}_{\hat\imath\,A}{}^B + \Gamma^{\hat\imath}{}_{\hat\nu\hat\mu}\,F^{(A,n)}\,V^{(n)}\,G^{\hat\nu\hat\mu}{}_{\hat\imath\,A}{}^B + \text{“energy coupling terms”} = \mathbb{S}^B}$$

- P, F, G: pure **angular-basis** integrals (and derivatives) → **precomputed once**
- $V^{(n)}$: the **energy-bin weight**, fixed by the energy grid → precomputed as well

You solve: $N_{\text{ang}} \times N_{\text{E}}$ coupled **3D advection equations** – one per mode (A, n) linked through the precomputed matrices above and the stiff matter-coupling source $\mathbb{S}^B$

Angular discretization

Consider for now, special relativity and no moving medium (Ω^i the unit propagation direction, $p^i = \varepsilon\,\Omega^i$):

$$M^B{}_A \frac{\partial F^A}{\partial t} + S^{iB}{}_A \frac{\partial F^A}{\partial x^i} = \mathbb{S}^B$$

mass matrix

$$M^B{}_A = \int \Psi^B \Psi_A \,\mathrm{d}\Omega$$

stiffness matrix

$$S^{iB}{}_A = \int \Omega^i\, \Psi^B \Psi_A \,\mathrm{d}\Omega$$

Both are pure angular integrals fixed once Ψ_A is chosen, only the collision integral $\mathbb{S}^B[F]$ needs recomputing every step. **[Bhattacharyya & Radice 2023]**

The choice of Ψ_A *is* the method: $Y_{lm} \Rightarrow$ **FP$_\mathrm{N}$** tent functions $\Rightarrow$ **FEM$_\mathrm{N}$** indicator functions $\Rightarrow$ **S$_\mathrm{N}$**

Geodesic grid

A local angular basis needs a mesh of $\mathbb{S}^2$. A naive (θ, ϕ) grid singles out an axis: cells shrink near poles – at poles a coordinate singularity: an unphysical preferred direction.

A geodesic grid avoids this!

Initial construction:

- base grid: the 12 vertices of a regular **icosahedron**, $\varphi = \frac{1+\sqrt{5}}{2}$,

$$\frac{1}{\sqrt{1+\varphi^2}}\left[(0,\pm1,\pm\varphi),\ (\pm1,\pm\varphi,0),\ (\pm\varphi,0,\pm1)\right]$$

  projected onto the unit sphere **[Giraldo 1997]**

- Refinement by **edge bisection**: insert the midpoint of every edge and project it back

$$\vec{x}_C = \frac{\vec{x}_A + \vec{x}_B}{2} \longrightarrow \frac{\vec{x}_C}{|\vec{x}_C|}$$

- triangular elements have more or less the same area: no cell ever shrinks to a point
- all vertices stored in **Cartesian** coordinates → avoids singularities at the poles, and no axis is preferred

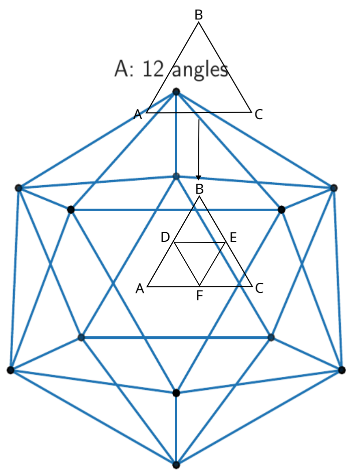

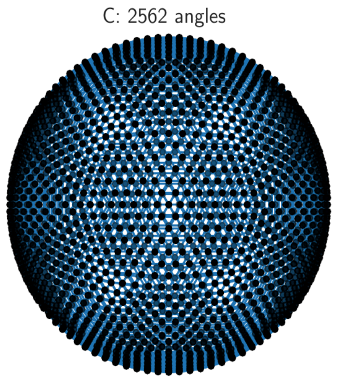

Basis functions on the geodesic grid — FEM_N and S_N

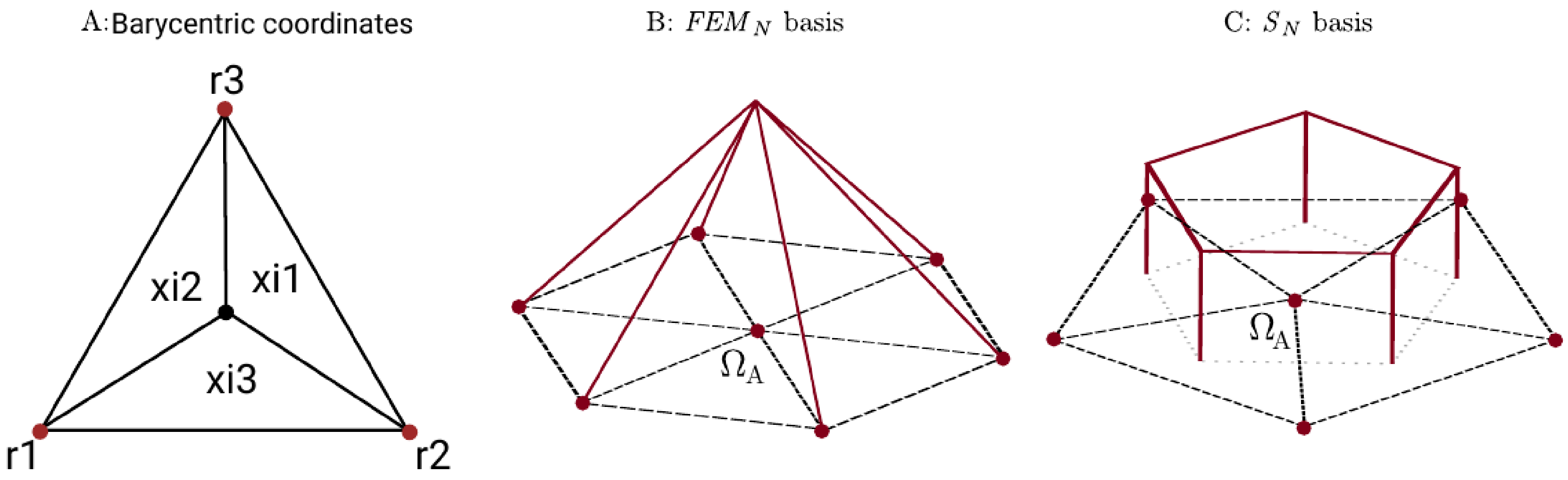

Barycentric (areal) coordinates locate a point as a weighted average of the triangle's vertices:

$$\mathbf{r} = \xi_1\mathbf{r}_1 + \xi_2\mathbf{r}_2 + \xi_3\mathbf{r}_3$$

$$\xi_1 + \xi_2 + \xi_3 = 1$$

each ξ_i equals the fractional area of the sub-triangle opposite vertex i.

FEM_N – overlapping "tent" functions, peaking at one vertex and vanishing at the others:

$$\Psi_A = 2\xi_1 + \xi_2 + \xi_3 - 1$$

continuous across elements → sparse matrices coupling neighbouring angles, and the mass matrix is **lumped**.

S_N – non-overlapping indicator ("honeycomb") functions:

$$\Psi_A = \begin{cases} 1, & \xi_1 \geq \xi_2 \text{ and } \xi_1 > \xi_3 \\ 0, & \text{otherwise} \end{cases}$$

discrete ordinates arise as a special case of the same framework.

Overlapping basis reduces ray effects – FEM_N splits a beam smoothly across multiple neighbours, while S_N's disjoint patches force it into one.

Filtered spherical harmonics

- $\Psi_A = Y_{lm}(\theta, \phi)$: orthonormal, spectral, eigenfunctions of the Laplace-Beltrami operator on $\mathbb{S}^2$

$$Y_{lm} = \sqrt{\tfrac{2l+1}{4\pi}}\, P_l^0(\cos\theta), \quad m = 0$$

$$Y_{lm} = \sqrt{\tfrac{2l+1}{2\pi}\tfrac{(l-m)!}{(l+m)!}}\, \cos(m\varphi)\, P_l^m(\cos\theta), \quad m > 0$$

$$Y_{lm} = \sqrt{\tfrac{2l+1}{2\pi}\tfrac{(l-|m|)!}{(l+|m|)!}}\, \sin(|m|\varphi)\, P_l^{|m|}(\cos\theta), \quad m < 0$$

- derivatives are computed using **recurrence relations**:

$$\frac{\partial Y_{lm}}{\partial\varphi} = -m\, Y_{l\,-m}$$

$$(1 - x^2)\,\frac{\mathrm{d}P_l^m}{\mathrm{d}x} = (l + m)\, P_{l-1}^m - l\, x\, P_l^m, \quad x = \cos\theta$$

quadrature is chosen so every product $Y_{lm}Y_{l'm'}$ integrates **exactly**

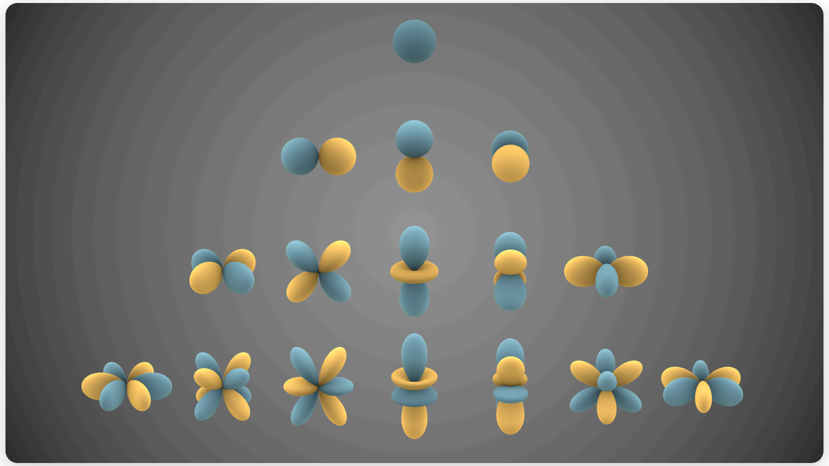

Real Y_{lm} on $\mathbb{S}^2$.

advantage: exactly rotationally invariant - no preferred directions, unlike $\mathrm{S_N}$

disadvantage: truncated expansions of sharp angular features oscillate (Gibbs phenomenon), $\mathrm{FP_N}$ handles beams/rays worse than $\mathrm{S_N}$

remedy → filtering

Positivity preservation

FP_N – filtering [Bhattacharyya & Radice 2023]

- damp every mode $A = \{l, m\}$ each sub-step, then reconstruct

$$F^{\text{new}} = \sum_A \sigma\left(\frac{l}{l_{\max}+1}\right)^s F^A Y_A$$

- the strength s is set by the effective opacity, $\sigma_{\text{eff}} \sim 5\text{-}50$ in practice, **problem-dependent** and must be tuned
- suppresses oscillations *and* genuine angular structure alike, negativity is reduced
- no guarantee but works in most cases

FEM_N – clipping limiter [Bhattacharyya & Radice 2023]

- clip the negative coefficients, $\tilde{F}^A = \max(F^A, 0)$, then rescale the survivors to conserve the energy density

$$\theta = \frac{\sum_{A,B} M_{AB} F^A}{\sum_{A,B} M_{AB} \tilde{F}^A}$$

- **parameter-free**, positivity-preserving, and conserves the density point-wise

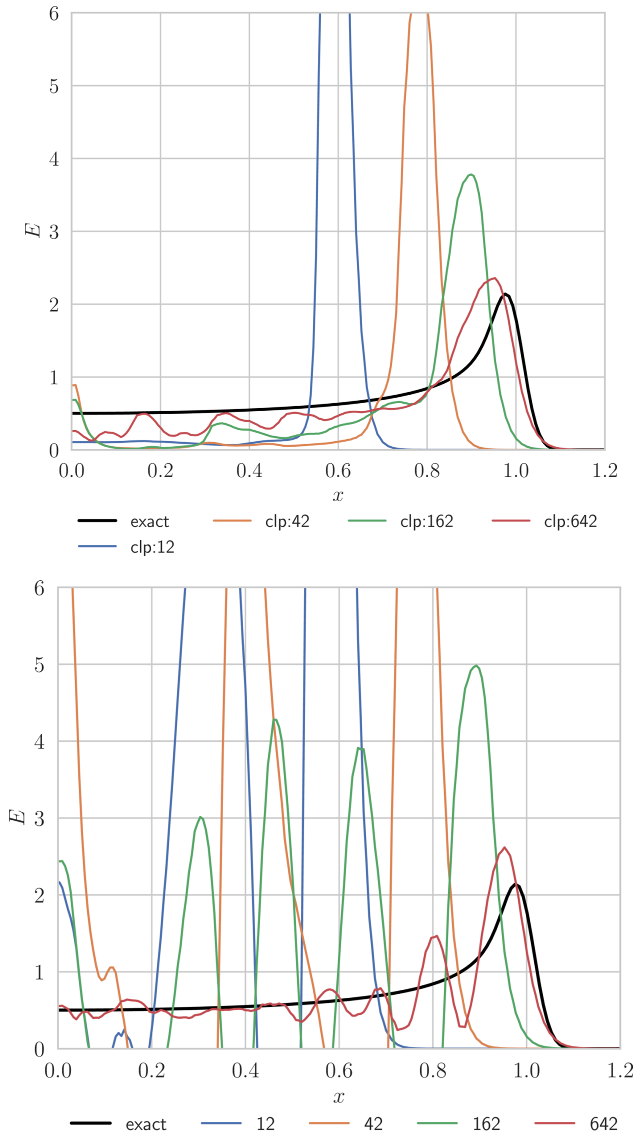

Line-source test, FEM_N at 12, 42, 162, 642 angles against the exact solution, with the clipping limiter (top) and without it (bottom). [Bhattacharyya & Radice 2023]

The diffusion limit

Recall $M^B{}_A\,\partial_t F^A + S^{iB}{}_A\,\partial_i F^A = \mathbb{S}^B$. FP_N $\to$ Truncate it to its first two moments in a static, purely scattering slab, the energy density $E \equiv F^0$ and the flux $F \equiv F^1$

$$\partial_t E + \partial_x F = 0, \qquad \partial_t F + \tfrac{1}{3}\partial_x E = -\tau^{-1} F$$

with τ^{-1} the scattering rate. This system is **hyperbolic**.

For $t \gg \tau$ the flux has time to relax between scatterings, $F \to -\frac{\tau}{3}\partial_x E$, and substituting turns the system into the heat equation

$$\partial_t E = \frac{\tau}{3}\,\partial_x^2 E$$

which is **parabolic**.

> The same equation changes character as the medium turns optically thick, and a scheme built only for the hyperbolic case does not see this on its own.

A scheme is **asymptotic-preserving (AP)** if its discrete diffusion rate stays correct even when the mean free path is unresolved, $c\tau \ll \Delta x$ [Larsen+ 1987, Lowrie & Morel 2002]. Standard hyperbolic solvers need Δx down near $c\tau$ to see this limit at all. The known exception among standard methods is **discontinuous Galerkin**.

Spatial discretization — asymptotic-preserving DG

1D case:

$$\frac{\partial F^A}{\partial t} + \tilde{S}^{xA}{}_B \frac{\partial F^B}{\partial x} = \mathbb{S}^A[F]$$

Pair cells (x_i, x_{i+1}) into an element $[x_{i-1/2}, x_{i+3/2}]$ $\rightarrow$ two linear basis functions reconstructing F from its values at the edges [Cockburn & Shu 2001, Radice+ 2013]

Time update built from the flux averages across the element $\bar{\mathcal{F}}$ and the **Riemann** flux at its own edges, $\mathcal{F}^-$ and $\mathcal{F}^+$

$$\frac{\mathrm{d}F_i^A}{\mathrm{d}t} = \frac{1}{\Delta x}\left(\tfrac{3}{2}\mathcal{F}^{-A} - \bar{\mathcal{F}}^A - \tfrac{1}{2}\mathcal{F}^{+A}\right), \qquad \bar{\mathcal{F}}^A = \tfrac{1}{2}\left(\tilde{S}^{xA}{}_B F_i^B + \tilde{S}^{xA}{}_B F_{i+1}^B\right)$$

Expanded, $\mathcal{F}^-$ and $\mathcal{F}^+$ pull in cell values from the neighboring elements on either side.

The Riemann flux still needs dissipation on **zero-speed modes** of $\tilde{S}^x$

$$\mathcal{F}^{-A} = \tfrac{1}{2}\left[\tilde{S}^{xA}{}_B(F_L^B + F_R^B) - \hat{S}^{xA}{}_B(F_R^B - F_L^B)\right], \qquad \hat{S}^{xA}{}_B = \mathcal{R}^{xA}{}_C \max\left(v, |\Lambda^{xC}{}_D|\right) \mathcal{L}^{xD}{}_B$$

with $v = \frac{1}{\sqrt{3}}$ a floor on the dissipation speed.

A minmod or double-minmod slope limiter keeps the solution monotone.

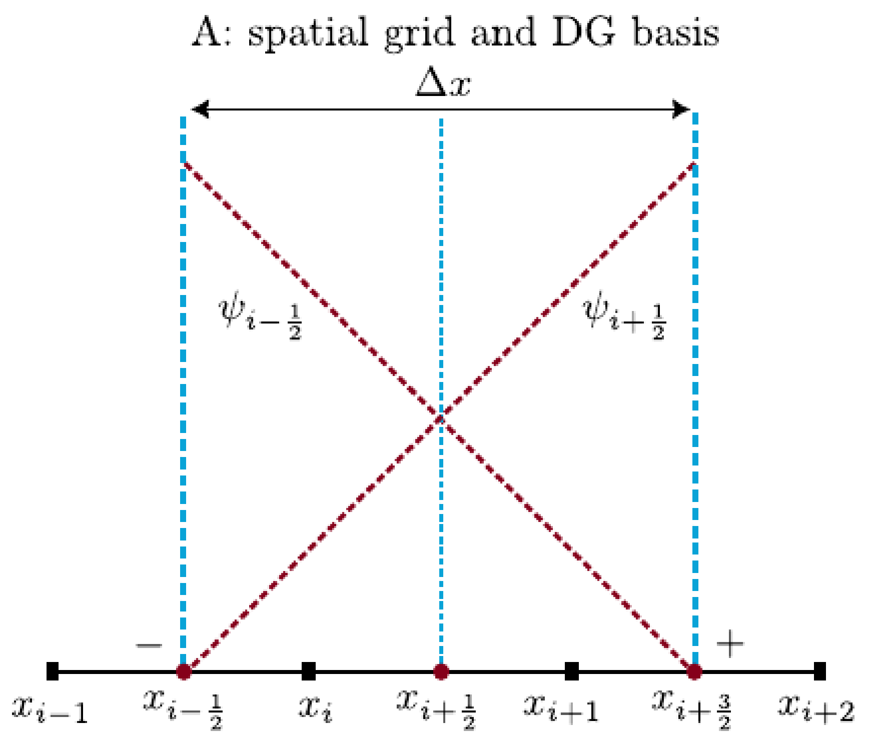

DG element, two cells sharing linear basis functions.

Time integration

The collision term from before splits into two pieces [Bhattacharyya & Radice 2023]

$$\mathbb{S}^A[F] = e^A + P^A{}_B\, F^B$$

- e^A: **emission term** $\to$ treat this explicitly!
- $P^A{}_B\, F^B$ collects **absorption and scattering**, both scaling as $1/\lambda$, so they turn stiff exactly where the mean free path shrinks

> Semi implicit scheme: The stiff linear term $P^A{}_B F^B$ needs an implicit solve. A scheme split: explicit for the cheap terms and implicit for the stiff one [McClarren+ 2008].

A **second-order Runge-Kutta** stepping realizes this split [Bhattacharyya & Radice 2023]

$$F^A_{k+1/2} = F^A_k - \frac{\Delta t}{2}\left(\tilde{S}^i{}_{BA}\partial_i F^A\Big|_k + e^A_k + P^A{}_B F^B_{k+1/2}\right)$$

$$F^A_{k+1} = F^A_k - \Delta t\left(\tilde{S}^i{}_{BA}\partial_i F^A\Big|_{k+1/2} + e^A_{k+1/2} + P^A{}_B F^B_{k+1}\right)$$

- solving for $P^A{}_B F^B$ is **local to each spatial element**, a small dense solve
- the $\mathrm{FP_N}$ filter and the $\mathrm{FEM_N}$ limiter are applied after each sub-step

Test: line source

A pulse of radiation concentrated on the z-axis expands into an isotropic ring [Ganapol 1999] – the standard probe of angular resolution and rotational invariance.

- **S_N** breaks the ring into discrete blobs – ray effects
- **FP_N** best for this test but admits small negative values which can be filtered away.
- **FEM_N** converges to the exact ring as N grows → middle ground

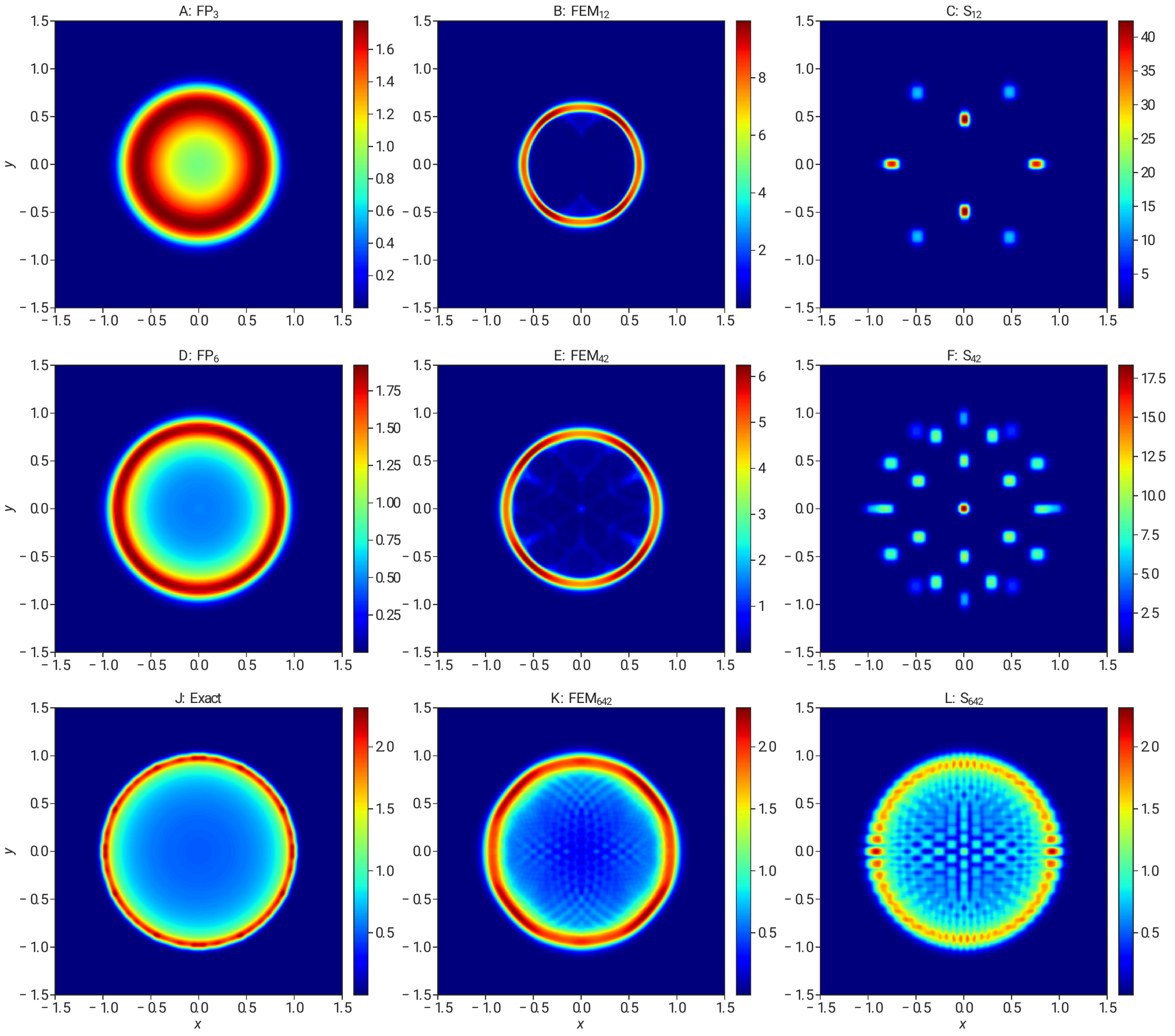

Line test for $FP_{3/6}$, $FEM_{12/42/642}$, $S_{12/42/642}$ against the exact solution (bottom left).

Test: lattice

An emitting core surrounded by absorbing and scattering blocks [Brunner 2002] – mixed optically thick and thin regions in a structured geometry.

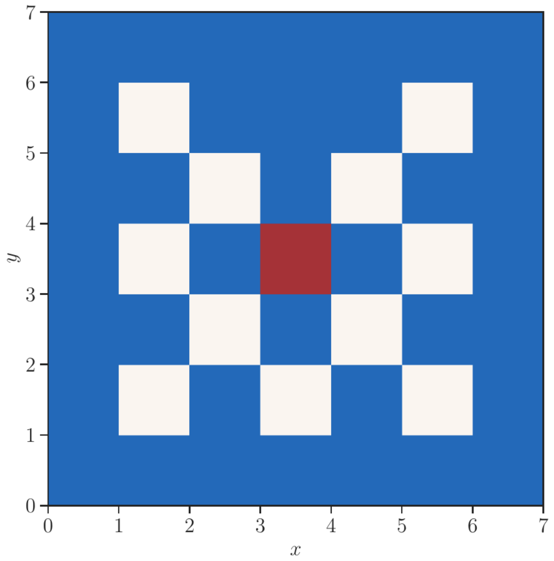

- central square **emits** ($\eta = 1/4\pi$) with scattering opacity $\kappa_s = 10$
- 11 blocks **absorb** ($\kappa_a = 1$) in a purely **scattering** ($\kappa_s = 1$) background
- **S_N** produces star-shaped ray artifacts, especially at low angular resolutions
- **FP_N** and **FEM_N** yield smooth, mutually consistent solutions

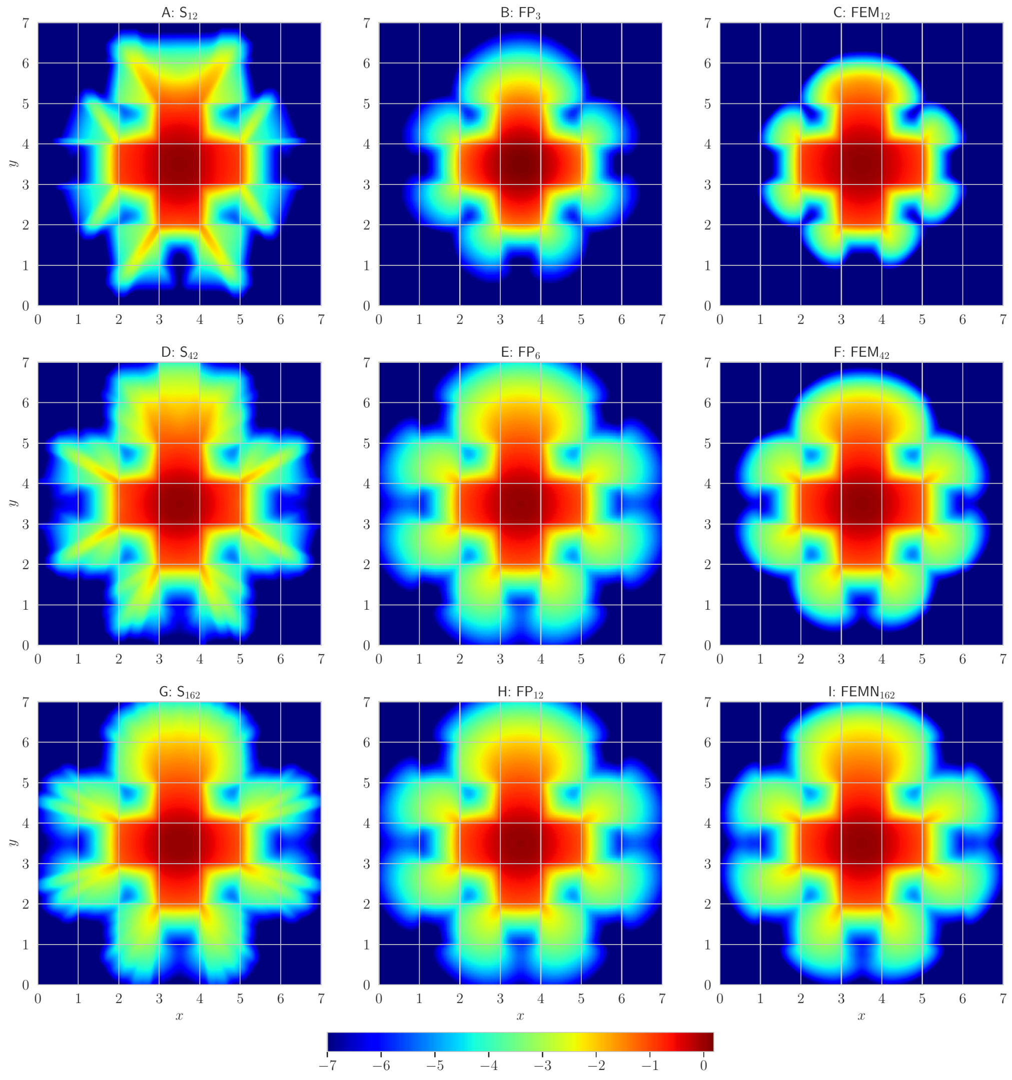

$\log_{10} E$ at $t = 3.2$: S_N stays “ray-like” even at 642 angles; FP_N and FEM_N reach comparable accuracy at high resolution. [Bhattacharyya & Radice 2023]

Test: lattice, steady state

Same setup, evolved further to $t = 16$ until the fields stop changing.

- **S_N** keeps its star-shaped ray artifacts even at 162 angles
- **FP_N** and **FEM_N** agree closely at both resolutions shown
- either basis is a safe choice for this test, S_N is not

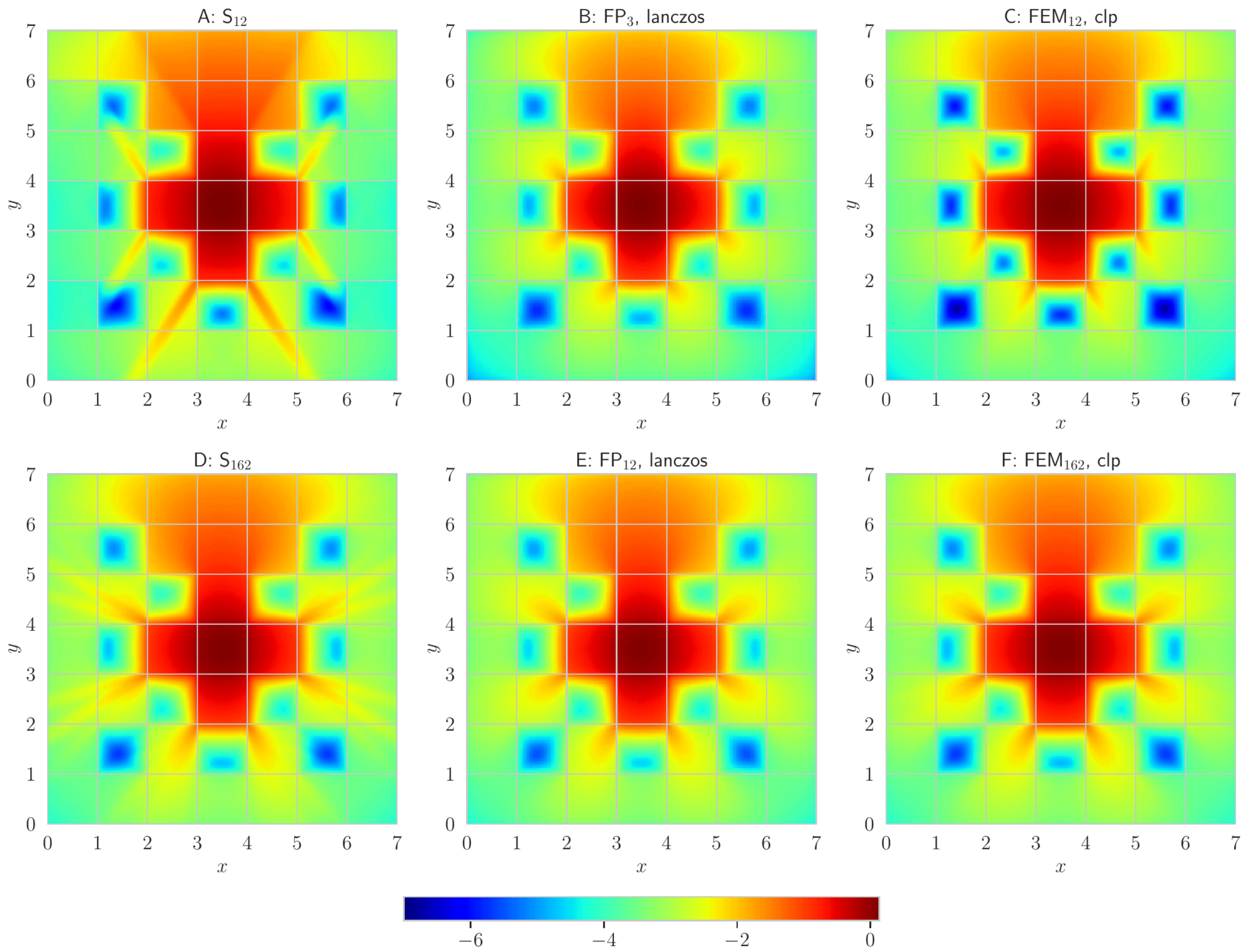

$\log_{10} E$ at steady state, S_N, FP_N, FEM_N at 12 angles (top) and 162 angles (bottom).

[Bhattacharyya & Radice 2023]

Test: Beams

Two narrow beams enter from the boundary and cross in vacuum **[Stone+ 1992]** — the sharpest test of positivity and angular locality.

The $\Gamma p p \partial_p F$ term at work: a beam **bends** in the gravitational field of a black hole.

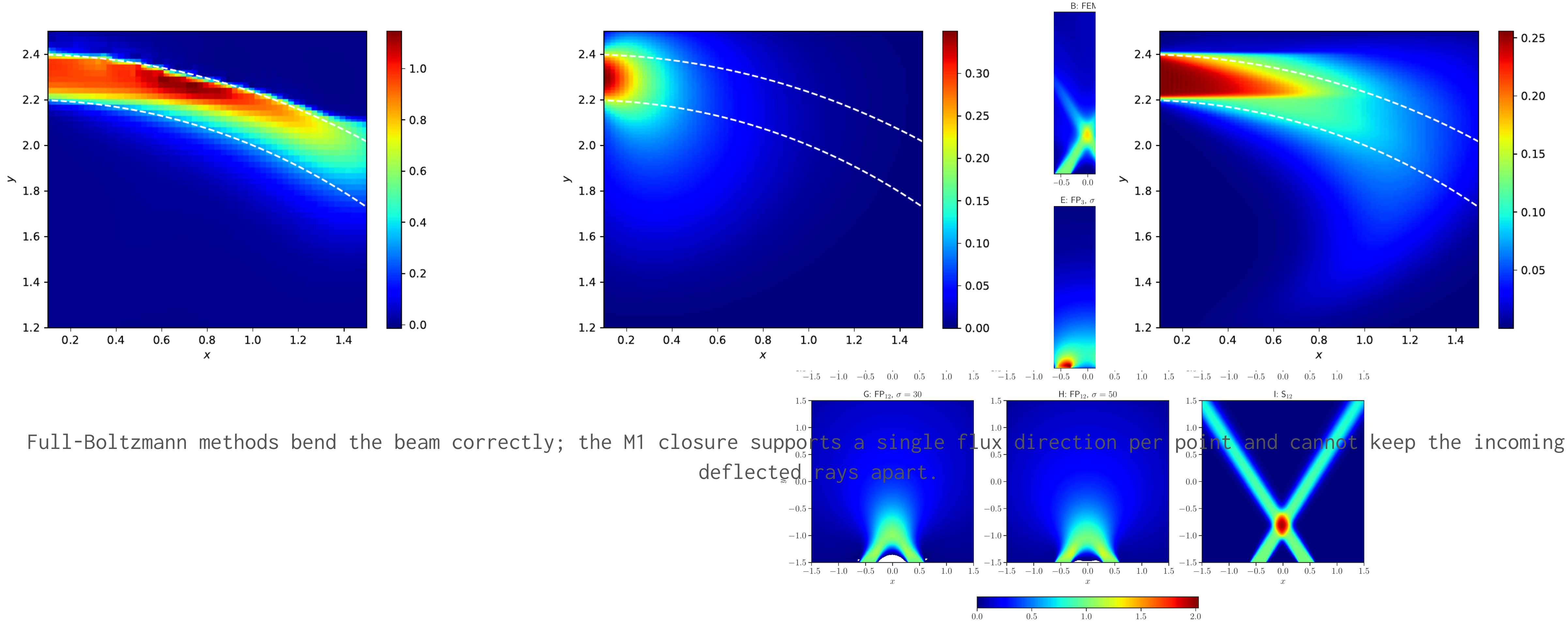

Full-Boltzmann methods bend the beam correctly; the M1 closure supports a single flux direction per point and cannot keep the incoming and deflected rays apart.

FEM$_{12-642}$ (top), FP$_{3-12}$ at varying filter strength σ, and S$_{12}$. White = negative.

Test: homogeneous cylinder

A unit-radius cylinder with uniform emissivity $\eta = 10$ and absorption $\kappa_a = 10$ sits in vacuum, no scattering. This is the classic **homogeneous sphere test**, generalized to two dimensions, a sharp discontinuity against a known analytic field [Bhattacharyya & Radice 2023]

Since $\eta = \kappa_a$, the source function is simply $S = \eta/\kappa_a = 1$. The domain spans $x, y \in [-2.5, 2.5]$ and is evolved to $t = 1.5$, just as radiation reaches the outer boundary.

- S_N shows pronounced flower-shaped ray artifacts even at 42 angles
- FP_N and FEM_N are already close to circular at low resolution
- all three schemes converge toward the correct circular front as the angular resolution grows

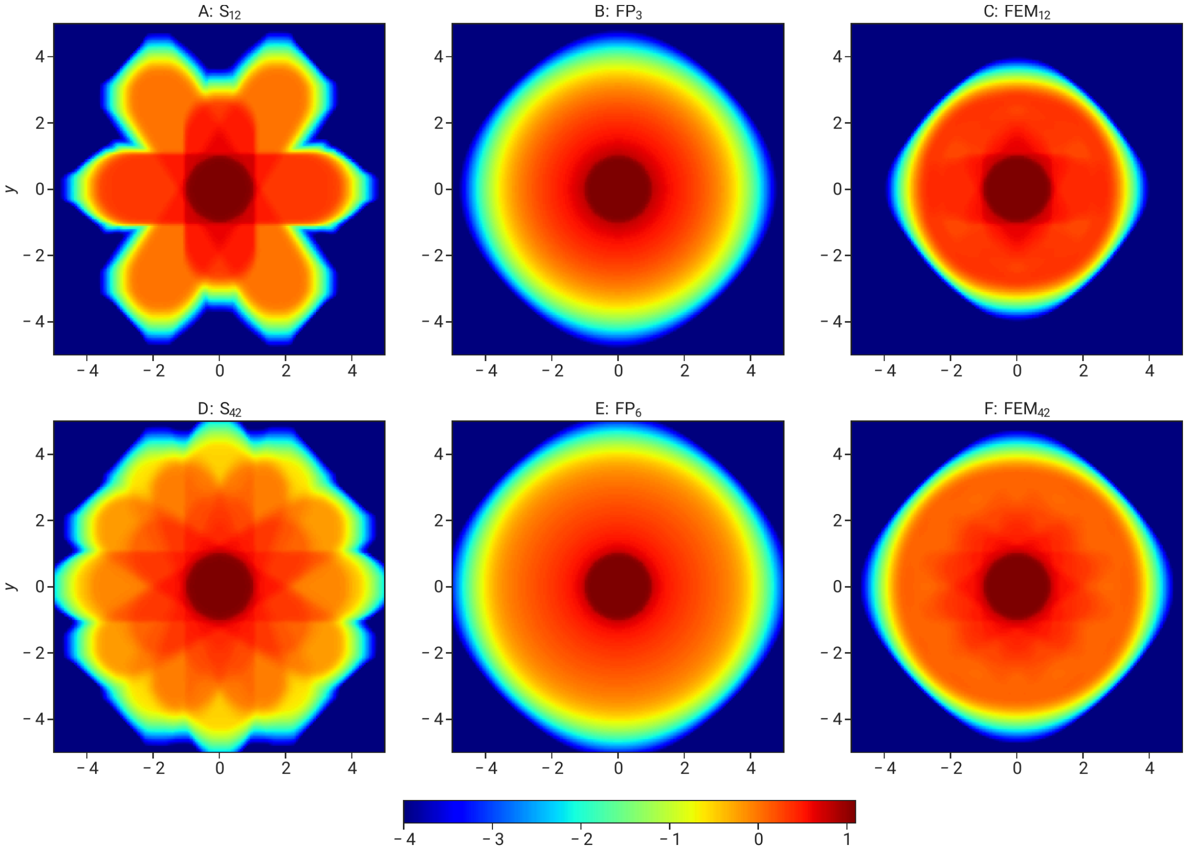

$\log_{10} E$ at $t = 1.5$, S_N, FP_N, FEM_N at 12 angles (top) and 42 angles (bottom). [Bhattacharyya & Radice 2023]

Test: cylinder, steady state

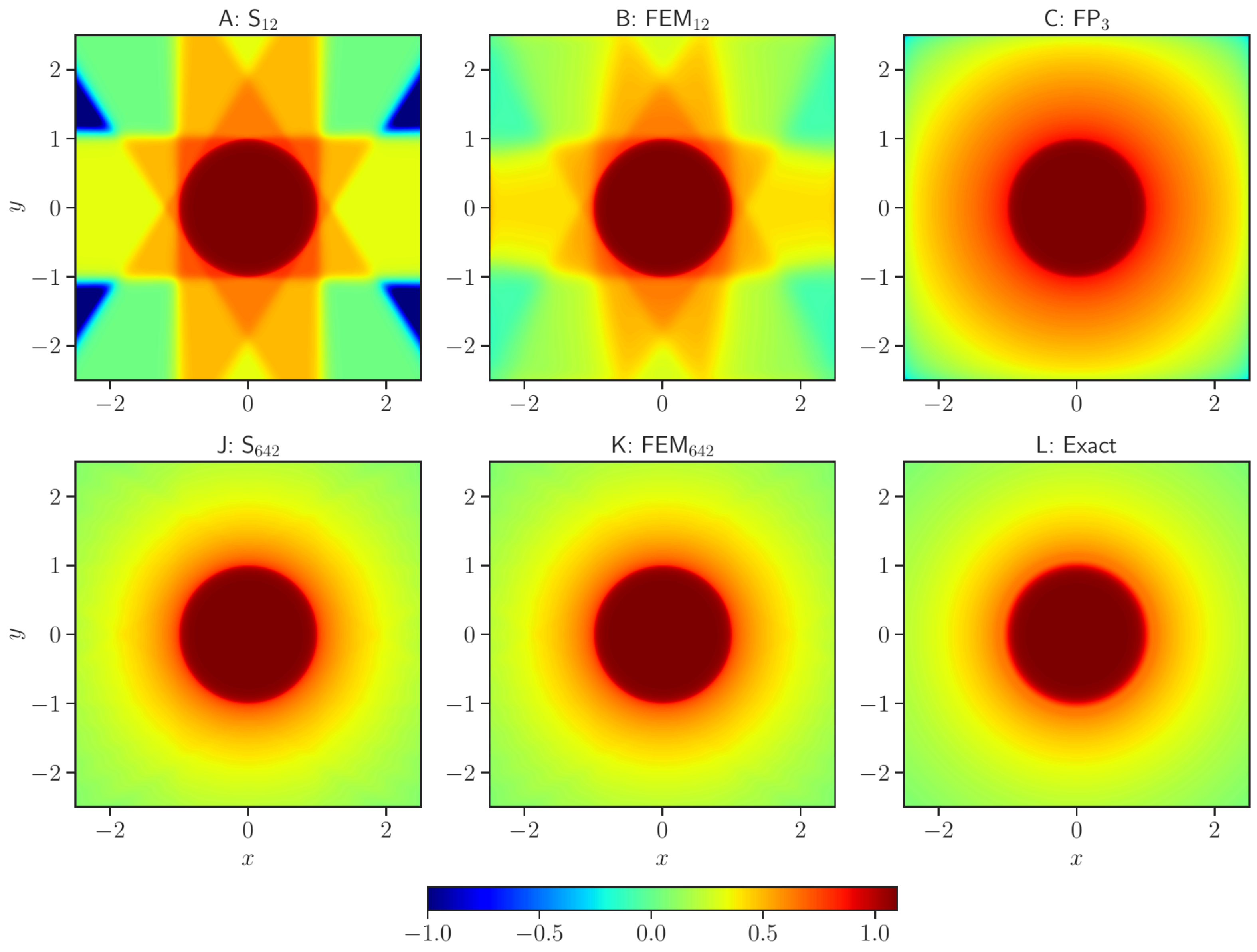

Test: cylinder, errors and convergence

The L^1 error against the exact solution,

$$\mathcal{E} = \frac{1}{N_p}\sum_i \left|E_i^{\text{exact}} - E_i^{\text{numerical}}\right|$$

is measured at three spatial resolutions, 150, 300, and 600 points per dimension [Bhattacharyya & Radice 2023]

- **$\mathrm{FEM_N}$** converges at close to first order in N, provided the spatial grid is fine enough
- at coarse spatial resolution the spatial error dominates, and refining the angular grid alone stops helping
- the largest error sits right at the cylinder's surface, where the field is discontinuous

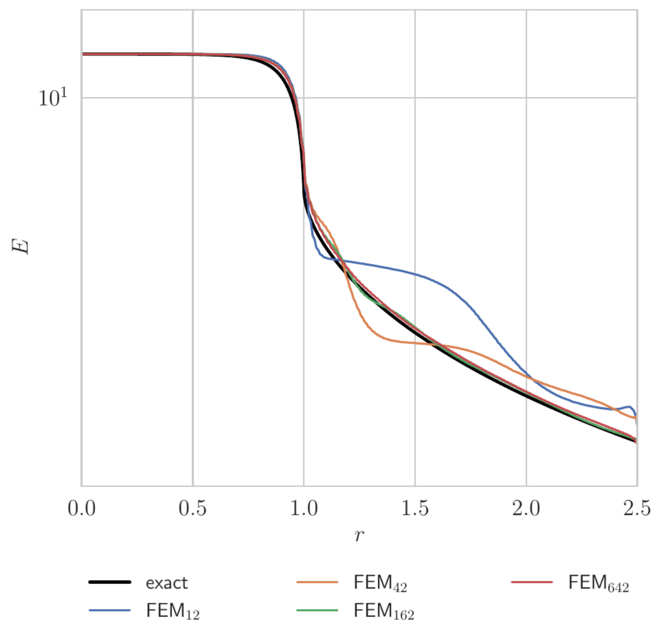

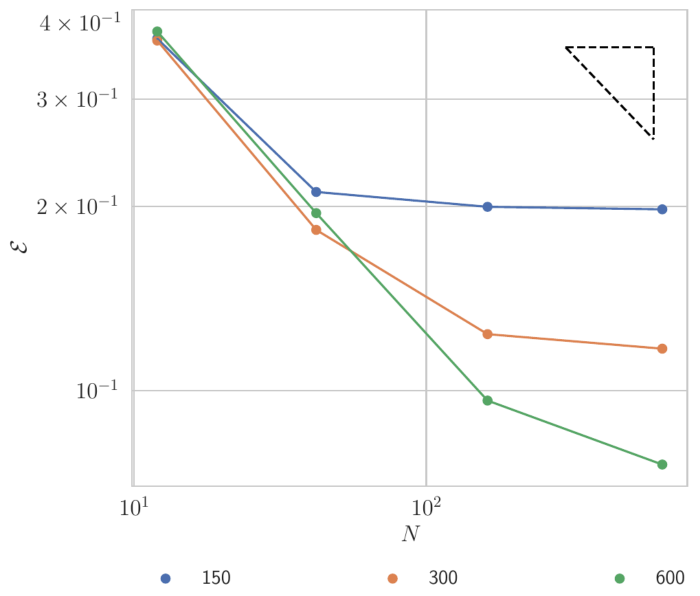

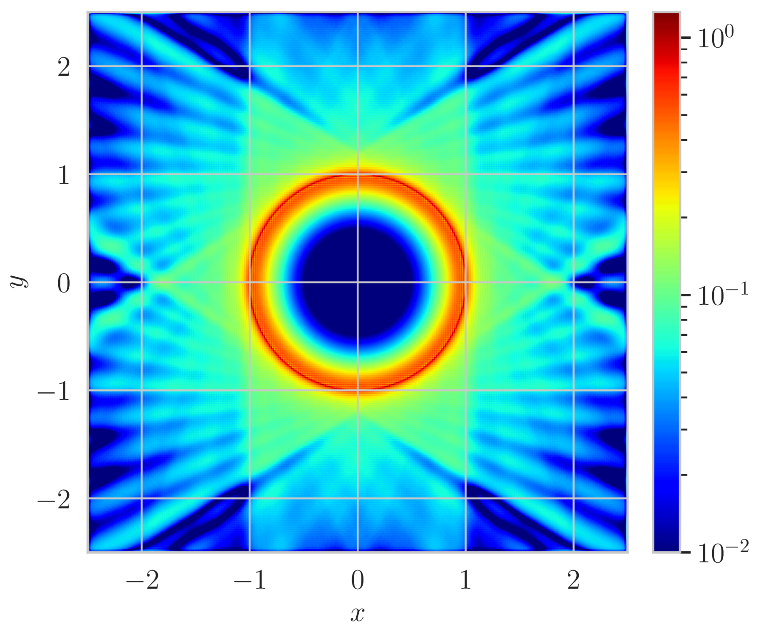

M1 transport

Decompose $T^{\mu\nu}$ with respect to the Eulerian observer [Shibata+ 2011]:

$$T^{\mu\nu} = E\, n^\mu n^\nu + F^\mu n^\nu + n^\mu F^\nu + P^{\mu\nu}$$

Then $\nabla_\mu T^{\mu\nu} = \mathcal{S}^\nu$ gives evolution equations for E and F_i:

$$\partial_t(\sqrt{\gamma}\,E) + \partial_i\big[\sqrt{\gamma}\,(\alpha F^i - \beta^i E)\big] = \alpha\sqrt{\gamma}\,\big[P^{ik}K_{ik} - F^i\partial_i \log\alpha - \mathcal{S}^\mu n_\mu\big]$$

$$\partial_t(\sqrt{\gamma}\,F_i) + \partial_k\big[\sqrt{\gamma}\,(\alpha P^k{}_i - \beta^k F_i)\big] = \sqrt{\gamma}\,\Big[-E\partial_i\alpha + F_k\partial_i\beta^k + \tfrac{\alpha}{2}P^{jk}\partial_i\gamma_{jk} + \alpha\mathcal{S}^\mu\gamma_{i\mu}\Big]$$

Two problems immediately appear:

1. we have no way to compute $P^k{}_i$ (**closure problem**)
2. the source term is only simple to compute in terms of fluid-frame moments,

   $$\mathcal{S}^\mu = (B - \lambda_a^{-1}J)\,u^\mu - (\lambda_a^{-1} + \lambda_s^{-1})\,H^\mu$$

   where B is the blackbody function, and the moments $\{J, H^\mu\}$ are implicitly defined by

   $$T^{\mu\nu} = J\,u^\mu u^\nu + H^\mu u^\nu + u^\mu H^\nu + K^{\mu\nu}$$

Note that $K^{\mu\nu}$ is the radiation pressure in the fluid frame, not the extrinsic curvature K_{ik} above.

The Minerbo closure

No algebraic closure $P^{ij} = f(E, F^i)$ can be exact! Pressure tensor depends on the full angular dependence, not just first two moments (E, F^i).

Minerbo's closure combines two known scenario: **isotropic**, where matter and radiation share a rest frame, and **free-streaming**, where radiation streams unimpeded from a point source [Minerbo 1978; Shibata+ 2011].

$$\boxed{K_{\alpha\beta} = \frac{3\chi - 1}{2} K_{\alpha\beta}^{\text{thin}} + \frac{3(1-\chi)}{2} K_{\alpha\beta}^{\text{thick}}}$$

$$K_{\alpha\beta}^{\text{thick}} = \tfrac{1}{3} J\,(u_\alpha u_\beta + g_{\alpha\beta}), \qquad K_{\alpha\beta}^{\text{thin}} = E\,\frac{F_\alpha F_\beta}{F_\mu F^\mu}$$

Eddington factor $\chi(\xi) = \dfrac{1}{3} + \xi^2 \dfrac{6 - 2\xi + 6\xi^2}{15}$ [$\frac{1}{3}$ to 1], with $\xi^2 = H^\mu H_\mu / J^2$ built from the **fluid-frame** flux F^μ

The cost:

1. finding ξ is an **implicit, nonlinear** solve, at every point, every step
2. a *linear* 6+1D equation has become a **nonlinear** 3+1D system
3. the closure feeds back into the source through $\{J, H^\mu\} = f(\{E, F^\mu\})$

Test: shadow and beam bending

Some examples:

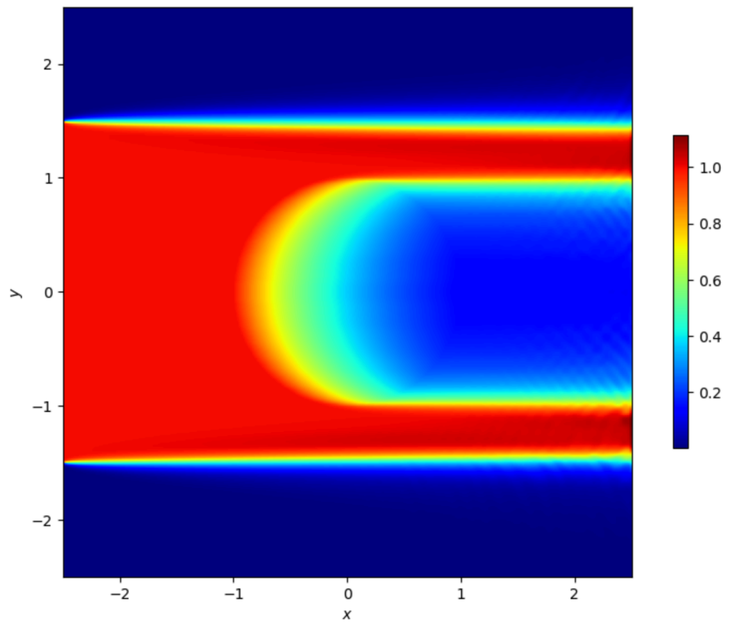

Energy density, beam strikes an absorbing sphere.

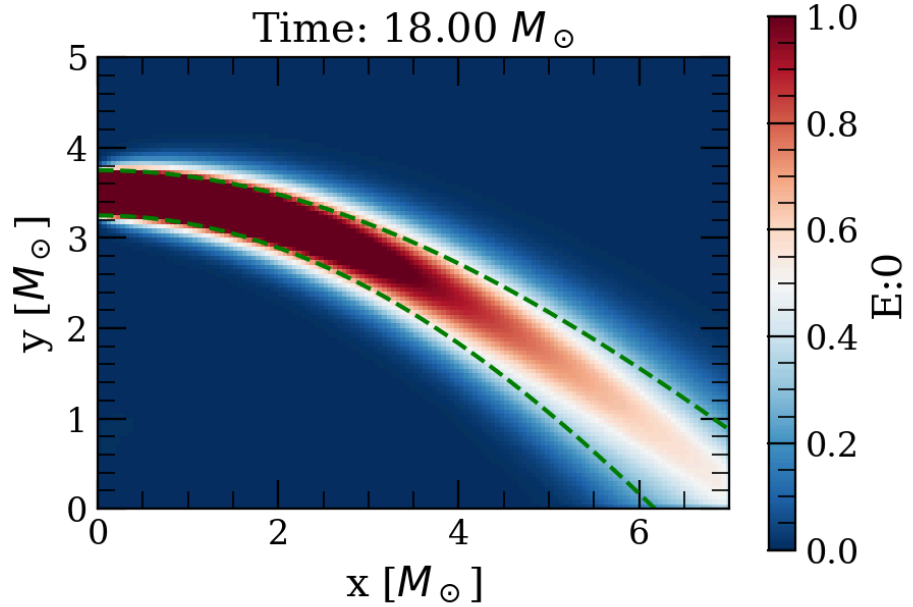

M1 energy density follows geodesic **[Yi Qiu]**

M1 + bns_nurates

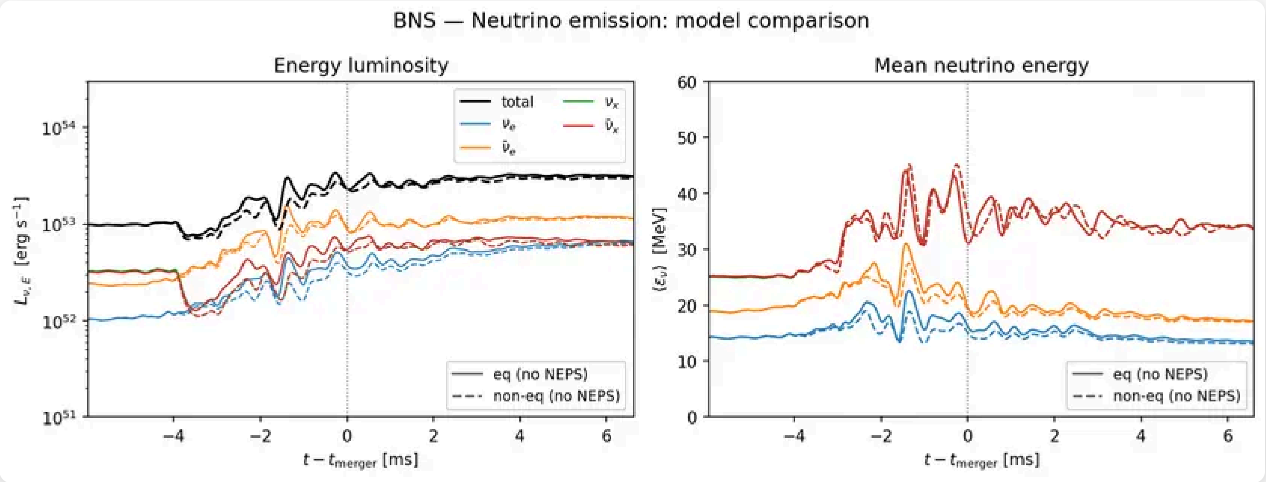

Neutrino luminosity and mean energy, extracted 300 km from the merger site **[Yi Qiu]**

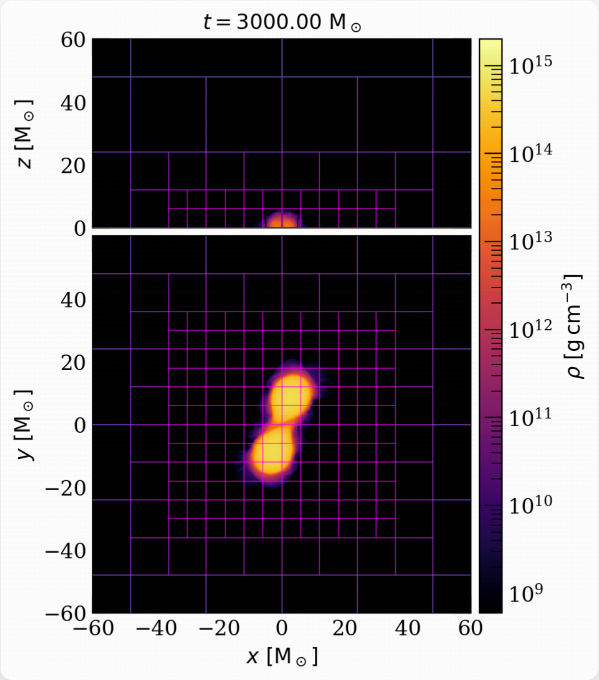

Rest-mass density through inspiral and merger, AthenaK M1 + bns_nurates **[Yi Qiu]**

Thank you

Maitraya Bhattacharyya
mabhattacharyya@mpia.de

Questions?

We acknowledge funding from the U.S. Department of Energy, Office of Science, Division of Nuclear Physics, under Award Numbers DE-SC0021177 and DE-SC0024388.